DOI: 10.13009/EUCASS2025-453
11TH EUROPEAN CONFERENCE FOR AERONAUTICS AND SPACE SCIENCES (EUCASS)

Turnaround and Refueling Analysis for Dual-Energy Carrier Aircraft

Jonas Mangold[⋆†] *and Andreas Strohmayer*[⋆]
[⋆]*University of Stuttgart, Institute of Aircraft Design*
Pfaffenwaldring 31, 70569 Stuttgart, Germany
mangold@ifb.uni-stuttgart.de · strohmayer@ifb.uni-stuttgart.de
[†]Corresponding author

Abstract

The integration of dual-energy carriers, which combine sustainable aviation fuels or liquid hydrogen with onboard batteries, into aircraft design and ground operations introduces new challenges for airport infrastructure and turnaround processes. Analyses indicate that achieving turnaround times competitive with conventional aircraft requires either rapid onboard charging at a C-rate of approximately $2.4\,\mathrm{h}^{-1}$ or battery swapping within 20 minutes. Liquid hydrogen refueling procedures are specifically scaled for smaller aircraft classes. A flexible, scalable methodology is developed, focusing on regional aviation. The findings underscore the need for a comprehensive approach that integrates aircraft design, ground operations, and infrastructure to ensure both economic and environmental viability.

1. Introduction

Air transportation supports economic growth and global connectivity by enabling fast travel and the transport of goods [1]. However, its environmental impact, including carbon dioxide, nitrogen oxide, and noise emissions, as well as contrails, has raised public concern. Climate change and regulations push the aviation sector towards more sustainable practices [1–3]. In this context, electrification and hybridization of propulsion architectures expand design possibilities for aircraft and propulsion systems, owing to the higher efficiency and mass-specific power of electric components [4, 5]. A hybrid-electric propulsion architecture with dual energy carriers can address the limited range of battery-electric aircraft – caused by the relatively low mass-specific energy of current battery technologies [4, 6, 7] – while also reducing fuel consumption and emissions [8–14], thus helping to meet stringent environmental targets.

Different propulsion architectures and energy carriers may be suited to various aircraft types and their projected availability [15]. Regional aircraft, in particular, offer greater potential for exploring alternative propulsion architectures and energy carriers [15]. In this context, dual-energy carrier aircraft can combine primary carriers – such as Sustainable Aviation Fuels (SAFs) or Liquid Hydrogen (LH2) – with electricity stored in batteries as a secondary energy source.

Beyond technical challenges such as installation and certification, the integration of dual-energy carriers necessitates modifications to aircraft turnaround and refueling processes. Turnaround time (TAT) significantly impacts aircraft competitiveness and revenue, which is typically assessed using Direct Operating Cost (DOC). DOC (see Equation 1) comprise per-flight costs for fuel (c_{fuel}), airport and route fees (c_{fees}), and maintenance (c_{maint}), as well as annual costs for crew (C_{crew}) and capital (C_{capital}) [16].

To enable comparability across different aircraft and missions, DOCs are normalized by the Available Seat Kilometer (ASK), which reflects costs per passenger-kilometer. The normalized DOCs, denoted as $\mathrm{DOC}_{\mathrm{ASK}}$, are calculated by dividing the total DOC by the product of flight range R and the number of passengers n_{PAX}. Additionally, annual costs are distributed across the number of Flight Cycles (FC).

$$\mathrm{DOC}_{\mathrm{ASK}} = \left(c_{\mathrm{fuel}} + c_{\mathrm{fees}} + c_{\mathrm{maint}} + \frac{C_{\mathrm{crew}} + C_{\mathrm{capital}}}{\mathrm{FC}} \right) / \left(R \cdot n_{\mathrm{PAX}} \right) \tag{1}$$

The number of FC also serves as an indicator of annual aircraft utilization (see Equation 2). It is determined by dividing the annual operating time $\mathrm{OT}_{\mathrm{p.a.}}$ by the sum of the Flight Time (FT) and a Block Time Supplement (BTS) [16]. As derived from Equation 2, for missions with short distances (i.e., short FT), such as those flown by regional or short-to-medium-range aircraft, BTS becomes comparable in magnitude to FT. In such cases, the TAT (represented by BTS) has a significant influence on aircraft utilization. To remain economically viable, commercial aircraft require high daily utilization [17]. Extended TATs reduce utilization, thereby increasing the cost per passenger-kilometer.

DOI: 10.13009/EUCASS2025-453

While an increased fleet size can compensate for longer TATs [18], this approach incurs additional capital and operational costs. For dual-energy carrier aircraft, these constraints necessitate adaptations to turnaround procedures, with corresponding implications for airport infrastructure and aircraft design.

$$\mathrm{FC} = \frac{\mathrm{OT}_{\mathrm{p.a.}}}{\mathrm{FT} + \mathrm{BTS}} \tag{2}$$

With the shift toward dual-energy carrier aircraft, two distinct energy sources must be exchanged during each turnaround: a primary energy carrier, such as SAFs or LH2, and a secondary energy carrier, namely electricity stored in batteries. Relevant characteristics and properties of these energy carriers are evaluated in Section 2.2. This dual-energy system introduces substantial complexity into refueling and turnaround operations, which are critical to aircraft utilization and economic viability. Aircraft designs should therefore also be optimized to minimize airport TAT – any solutions that reduce charging and refueling durations and enable greater aircraft utilization are preferable [19]. Consequently, this research addresses the resulting operational, design, and infrastructural implications of implementing dual-energy systems in future aircraft configurations.

The need to manage both SAF/LH2 refueling and battery charging or swapping within a constrained turnaround window presents a complex systems-level challenge, underscoring the necessity of a holistic design approach. The central hypothesis of this paper is that turnaround processes, refueling strategies, and aircraft design are strongly interdependent and must be addressed together to achieve a viable dual-energy carrier aircraft concept. This necessitates a multi-scale design approach – applicable not only to regional aircraft but extending from unmanned aerial vehicles to long-range aircraft. Development efforts should prioritize systems that enhance energy efficiency, safety, and reliability while minimizing TATs [19]. Traditional sequential design methods are inadequate for incorporating new propulsion technologies and energy carriers into early design phases. This research highlights the importance of evaluating not only the potential benefits, such as reduced fuel consumption and emissions, but also the operational and economic implications of dual-energy carrier aircraft. It focuses on identifying key turnaround requirements, ground energy supply, and design interdependencies that influence the viability and integration of such propulsion systems.

In Section 2, this paper presents the relevant fundamentals and state of the art necessary for reviewing the requirements of conventional aircraft turnaround and for integrating future energy carriers. Then, in Section 3, the methodology is described to analyze the required conditions for a competitive dual-energy aircraft. Finally, the results of the turnaround and refueling analysis, including airport infrastructure requirements, are given in Section 4.

2. Fundamentals

This section examines current operations with conventional aircraft and the relevant properties of various energy carriers to identify key influencing factors and define boundary conditions for the subsequent analysis. It begins with an overview of aircraft utilization and turnaround procedures, highlighting their economic implications. Next, the characteristics of the energy carriers – Jet A-1, SAFs, and LH2 as primary carriers, and battery-electric storage as a secondary carrier – are evaluated concerning their integration into turnaround processes and associated time constraints. The insights gained form the basis for assessing the compatibility of alternative propulsion architectures with dual-energy carriers.

2.1 Utilization and Turnaround Analysis of Conventional Aircraft

As previously introduced, aircraft utilization has a significant impact on the cost per available seat-kilometer. Figure 1 illustrates the influence of TAT and flight distance (i.e., FT) on annual FC. The curves indicate that increased TAT reduces the number of achievable flights per year, particularly for regional and short-to-medium-range aircraft operations – a finding consistent with earlier analysis.

Notably, aircraft availability exceeds actual utilization, indicating unused operational capacity. This gap may arise from scheduling constraints such as night flight bans. For dual-energy carrier aircraft, this discrepancy imposes additional constraints on operational feasibility. For regional aircraft with typical ranges around 500 NM [15, 20, 21], increasing the TAT from 25 min to 55 min results in decrease of the utilization to 75 %, as shown in Figure 1.

Assuming that fuel and crew costs each contribute one-sixth, and capital costs one-third of the direct operating costs (DOCs) (see Equation 1), achieving cost parity under extended turnaround times – rising from 25 to 55 minutes – would necessitate an unrealistic 100 % reduction in fuel costs or, alternatively, a significant decrease of one-sixth across all remaining cost components.

DOI: 10.13009/EUCASS2025-453

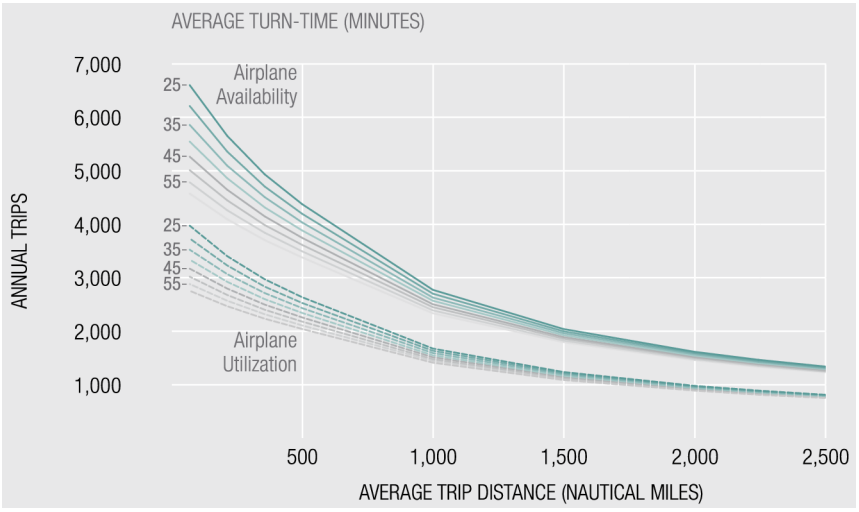

Figure 1: Airplane availability and utilization as a function of average trip distance and turnaround time [22]

TAT is defined as the interval between the actual arrival and actual departure time of the aircraft [23]. Alternatively, it is measured between on-block (wheel chocks in) and off-block times [24, 25]. TAT comprises several subprocesses – deboarding, unloading, fueling, cleaning, catering, loading, and boarding – which may occur in parallel or sequence, depending on logistical and regulatory factors. Typical TATs vary by aircraft type: approximately 17 min for regional, 35 min for single-aisle, and 61 min for twin-aisle aircraft [25]. The critical path, which is the longest sequence of dependent processes, determines the minimum achievable TAT and heavily influences short-haul utilization. The business model of the airline (e.g., low-cost vs. full-service carriers) also shapes TAT [26]. Fuel handling regulations further affect TAT. Jet A-1 refueling is allowed with passengers onboard, subject to operational procedures with passengers embarking, onboard, or disembarking [27]. If refueling lies on the critical path, such restrictions can significantly impact TAT and overall aircraft performance.

2.2 Relevant Characteristics of Energy Carriers

This section introduces the properties of fuels and energy carriers relevant for future aircraft configurations. Firstly, the differences and similarities between Jet A-1 and the carbon-neutral SAFs are evaluated. Secondly, the properties of LH2 are reviewed, along with a qualitative description of the associated refueling procedures. Finally, the properties of batteries will be elaborated. However, it is of major importance that the production of future energy carriers, such as SAF, LH2, and the electricity for batteries, is based on environmentally friendly, renewable energy.

2.2.1 Jet A-1 and Sustainable Aviation Fuels

Modern jet aircraft almost exclusively use Jet A-1, offering a high mass-specific energy of 12.0 kWh/kg and a volume-specific energy of 9.2 to 10.0 kWh/l at a density of 775 to 840 kg/m^3 [28, 29]. Its broad liquid temperature range (−47 to 38 °C) enables wing storage without complex insulation [28]. Jet fuels must meet strict criteria for energy density, thermal stability, flash point, lubricity, and material compatibility [30, 31]. Jet A-1 consists mainly of alkanes, cycloalkanes, and aromatics (improving seal performance and reducing leakage) [30]. Standards such as ASTM D1655-09 and Def Stan 91-91 govern fuel system compatibility [31]. Aviation fuel also supports heat management and mass balancing during flight [31].

SAFs are renewable drop-in alternatives produced via bio-based or synthetic pathways (e.g., Fischer-Tropsch) [30, 32]. Despite their chemical similarity to Jet A-1, SAFs must meet the same specifications to ensure full compatibility [31, 33]. SAFs offer reduced lifecycle emissions and contrail formation potential [34], but current production remains limited and energy-intensive [34, 35]. As a near-term solution, SAFs require minimal infrastructure changes and align with existing refueling procedures [5].

Commercial aircraft are typically refueled via underwing single- or dual-point connections using trucks or dispensers. Connection and disconnection generally require approximately 2.5 minutes [36]. Dual-side refueling is common for long-range aircraft to reduce TATs, enabling flow rates of up to 3600 l/min, corresponding to an energy transfer of approximately 583 kWh/s. However, flow rates are limited by electrostatic charge buildup during fuel transfer, which can pose ignition hazards [37–39]. These risks are typically evaluated using a simplified Reynolds number to ensure safe operating conditions [40].

DOI: 10.13009/EUCASS2025-453

2.2.2 Hydrogen

Hydrogen has gained considerable attention in the transportation and energy sectors due to its carbon-free molecular structure, which enables operation without carbon dioxide emissions. In thermodynamic terms, equilibrium hydrogen refers to a mixture composed of parahydrogen (99.8 %) in its liquid state [41]. For the physical properties of parahydrogen, refer to the RefProp database [42]. Hydrogen exhibits a high mass-specific energy of 33.3 kWh/kg [43]. However, its low volume-specific energy limits its practical use in compact applications. At ambient pressure and a boiling point of 20.2 K, LH2 has a density of 70.8 kg/m^3 [44, 45], resulting in a volumetric energy density of approximately 2.4 kWh/l. Cryogenic storage introduces significant system complexity, requiring specialized materials to prevent leakage and embrittlement [46, 47], as well as vacuum-insulated or foam-insulated tanks to reduce boil-off [48].

In contrast, LH2 necessitates cryogenic storage, additional supply chain [49–51], and extensive redesign of onboard fuel tanks and systems [48]. The operational complexity of handling cryogenic fluids significantly affects turnaround procedures and airport compatibility, including the need for high insulation, boil-off management, and strict safety protocols [40, 52]. LH2 refueling demands dedicated airport infrastructure, specialized ground support equipment, and additional personnel training, all of which may negatively impact TATs and operational feasibility [20, 40, 48, 52]. For detailed analysis of LH2 aircraft refueling it is refereed to Mangold et al. [40, 52]: The refueling procedures are described and evaluated, considering the process steps connecting/disconnecting (each 2.5 min), purging (1.5 min), chill-down (1.0 min) and refueling with 20 kg/s (equivalent to 583 kWh/s) [40, 52]. The aircraft-airport interface consists of two connections: one for LH2 delivery with an inner diameter of 152.4 mm, and another for recovering vaporized gaseous hydrogen with an inner diameter of 127.0 mm [40, 52]. Both connections are ideally implemented using clean-break disconnects to avoid the need for costly helium purging [40, 52].

2.2.3 Battery

Batteries differ fundamentally from conventional fuels in that they integrate both energy storage and power delivery within a single system. In contrast, traditional propulsion systems decouple these aspects: fuel serves solely as an energy storage medium, while an engine provides power or thrust output. This intrinsic coupling in batteries is effectively illustrated using the Ragone diagram, which shows the trade-off between mass-specific energy E_S and mass-specific power P_S [53,54]. Depending on the cell technology and future advancements, batteries currently achieve mass-specific energy densities between approximately 0.2 and 0.6 kWh/kg [55]. In this study, a battery cell refers to an individual electrochemical unit, whereas a battery or battery pack denotes the assembly of multiple such cells.

The number of cells connected in series, $N_{\text{cell,s}}$, is determined by the ratio of the nominal battery voltage $V_{\text{bat,nom}}$ to the nominal voltage of a single cell $V_{\text{cell,nom}}$ [56, 57]. The number of parallel-connected cells, $N_{\text{cell,p}}$, must satisfy both the power and energy requirements. It is estimated as the maximum of the energy-based and power-based configurations, which depend on the maximum battery power $P_{\text{bat,max}}$, nominal capacity of a single cell $C_{\text{cell,nom}}$ and maximum C-rate $C_{\text{rate,max}}$. An important metric in battery operation is the C-rate, denoted as C_{rate}, which expresses the rate of charge or discharge current I relative to the nominal capacity C_{nom}:

$$C_{\text{rate}} = \frac{I}{C_{\text{nom}}} \tag{3}$$

Higher C-rates correspond to faster charging or discharging, thus enabling greater power delivery. The maximum C-rate $C_{\text{rate,max}}$ is constrained by thermal limits and the electrochemical stability of the cell and can be related to the maximum mass-specific power $P_{\text{S,max}}$ and energy $E_{\text{S,max}}$, by applying the relationships $P = V \cdot I$ and $E = C \cdot V$:

$$C_{\text{rate,max}} = \frac{P_{S,\text{max}}}{E_{S,\text{max}}} \tag{4}$$

In practice, battery systems are sized according to the required total energy and power at the system level. However, since P_S and E_S are intrinsically linked through the C-rate, battery pack design must carefully balance these parameters. During operation, battery cells generate heat due to internal losses.

According to the model introduced by Bernardi et al. [58], the total heat generation $\dot{Q}_{\text{bat,heat}}$ (see Equation 5) consists of irreversible Joule heating and reversible entropic heat. At high C-rates – and thus high currents – the reversible entropic component is typically negligible compared to resistive losses and can therefore be omitted [59]. The internal resistance of the battery pack, $R_{\text{i,bat}}$, depends on the single-cell resistance, $R_{\text{i,cell}}$, which varies with the state of charge (SOC), temperature, and whether the battery is charging or discharging [60, 61], as well as on the configuration of cells in series and parallel.

$$\dot{Q}_{\text{bat,heat}} = {I_{\text{bat}}}^2 \cdot R_{\text{i,bat}} = \left(C_{\text{rate}} \cdot \frac{E}{U}\right)^2 \cdot R_{\text{i,bat}} \tag{5}$$

DOI: 10.13009/EUCASS2025-453

2.3 Aircraft Classification by Energy Hybridization

To comprehensively evaluate the operational and infrastructural requirements of battery swapping, fast charging, and hydrogen refueling, aircraft must be classified according to their size, energy requirement and degree of electrification. The primary metric for this classification is the hybridization factor of energy H_E, which denotes the proportion of mission energy supplied by the electric powertrain. While the hybridization factor of power H_P represents the share of maximum propulsion power delivered electrically, it is of secondary importance when focusing on energy carrier ground supply, which is primarily governed by energy throughput.

These hybridization factors are beneficial for comparing various propulsion architectures, as they quantify both the ratio of electrical power (H_P) and the degree to which batteries are utilized as energy carriers (H_E) [62, 63].

Table 1: Aircraft class categorization by hybridization factor of energy

Aircraft Class	**Representative**	**MTOM** in kg	**Energy** in kWh	H_E in %	**Battery** in kg
UAV	Amazon Delivery Drone	40	0.4	100	1.7
Light Manned Aircraft	e-Genius	910	56	100	290
General Aviation	Cessna 208	3960	4105	10	875
Regional Aircraft	ATR 42	18600	11700	5–30	up to 4200

This section presents a comparative analysis of four representative aircraft classes: Unmanned Aerial Vehicles (UAVs), light manned aircraft, General Aviation (GA), and regional aircraft. Each class is represented by a current or conventionally representative, providing a reference for estimating relevant hybridization parameters.

An Amazon delivery drone serves as a reference for battery-electric UAVs [64]. With a battery mass of 1.7 kg [65] and a maximum take-off mass (MTOM) of 40 kg [64], it achieves full electrification of both energy and power domains, i.e., $H_E = H_P = 100\,\%$. UAVs are particularly interesting for studying charging and battery-swapping concepts, as their typical mission durations are relatively short – often under 30 minutes [65,66]. This limited flight time allows for highly predictable energy demands and frequent turnaround cycles, making them well-suited for automated ground energy supply solutions.

The e-Genius aircraft [67], developed by the University of Stuttgart, exemplifies a fully electric light manned aircraft. With an MTOM of 910 kg and a battery mass of 290 kg [67], it likewise achieves full electrification ($H_E = H_P = 100\,\%$). This class is suited for piloted flight demonstrations.

The Cessna 208 Caravan is used as a representative GA aircraft, modified for hybrid-electric propulsion to estimate relevant hybridization parameters. Conventionally fueled with 1008 kg of Jet-A [68], and assuming a combustion efficiency of 35 % [4], the usable propulsion energy equates to approximately 4105 kWh. A hybridization factor of $H_E = 10\,\%$ implies an electric energy share of about 437 kWh. Assuming a specific energy of 500 Wh/kg, the corresponding battery mass is estimated at 875 kg. The partial hybridization of such aircraft introduces logistical challenges: batteries must be integrated modularly and exchanged or recharged within turnaround constraints. As the electric system complements conventional propulsion, ground infrastructure must support both energy carriers.

For the regional aircraft class, the ATR42 [69] serves as a reference platform for defining hybridization parameters. Assuming a fixed power hybridization of $H_P = 20\,\%$, the resulting energy hybridization factor H_E ranges between 5 % and 30 %, depending on the applied energy management strategy (see Section 3.5). A summary of key aircraft parameters is presented in Table 1.

Aircraft larger than the regional class are excluded from this analysis. For these, LH2 and SAF refueling are already studied, and the required battery mass for full electrification remains infeasible with current battery technology [15]. Thus, this classification provides a structured framework for investigating the integration of dual-energy aircraft, encompassing hybrid-electric and hydrogen-based propulsion, across various scalable aircraft categories. It supports the development of tailored infrastructure and operational concepts that meet both technical and regulatory requirements.

3. Methodology

A structured methodology is developed to assess the turnaround process of hybrid-electric aircraft with dual energy carriers. It defines boundary conditions to ensure competitive turnaround performance, followed by scaling laws for LH2 mass flow and the analysis for the battery ground energy supply. Battery charging constraints are integrated into a preliminary aircraft design tool, enabling sensitivity analyses under realistic operational conditions.

DOI: 10.13009/EUCASS2025-453

3.1 Boundary Conditions and Requirements

To ensure competitive aircraft operations, the TAT of hybrid-electric aircraft must not exceed that of conventional aircraft (see Section 2.1). Maintaining standard TATs is essential to preserve operational efficiency, maximize aircraft utilization, and ensure airline profitability. Therefore, energy supply processes – whether through battery charging, battery swapping, or refueling with SAF or LH2 – must be completed within this time frame.

An analysis of 13000 scheduled regional aircraft flights shows that approximately 49 % of turnarounds occur within 30 to 50 min, while 46 % exceed 50 min [70]. This identifies the 30 to 50 min minute window as the most critical scenario for ensuring turnaround compatibility in regional operations. Accordingly, a conservative TAT of 30 min is adopted as a boundary condition for the design and feasibility assessment of regional aircraft. Nevertheless, the proposed methodology allows for evaluating a wide range of TATs, enabling its application to different flight schedules and operational scenarios.

Consequently, all ground energy supply processes must be designed to operate within these constraints. This requirement directly informs the methodology and the scaling laws for battery charging, battery swapping, and LH2 refueling presented in the subsequent sections. If the required procedures – particularly those associated with dual-energy carrier systems – cannot be performed in parallel and must be executed sequentially, the TAT may increase significantly. Therefore, the potential for parallelizing ground handling processes is a critical aspect that must be carefully evaluated.

3.2 Scaling Laws for Liquid Hydrogen Refueling

Aircraft LH2 refueling infrastructure, and the majority of related research, is primarily focused on medium to large aircraft, where commercial business cases drive flow rates, pipe diameters, and technical capabilities. As shown in Mangold et al. [40, 52], refueling systems for regional and larger aircraft typically employ a main supply line with an inner diameter of 152.4 mm (6 in). This dimension ensures sufficiently high mass flow rates, for example up to 20 kg/s.

However, applying such large-scale systems to smaller aircraft categories – including GA, light manned aircraft, and UAVs – is infeasible due to significantly reduced hydrogen mass requirements and physical constraints, particularly the limited size of these vehicles. A direct (linear) downscaling of commercial systems is not practical, as hose dimensions and flow characteristics would become disproportionate. Instead, a systematic, dimensionless scaling approach must be employed to derive appropriate refueling parameters for these aircraft classes.

The principal constraint for LH2 pipe and flow design is an empirical upper limit for the product of flow velocity v and inner pipe diameter d, which serves as a simplified, dimensionless approximation of the Reynolds number [40]:

$$v \cdot d \quad \leq \quad 2.35\,\mathrm{m^2/s} \tag{6}$$

Additionally, the maximum permissible velocity depends on the length of the pipe. For short refueling hoses and long fixed pipelines at the airport, the following limits apply [40]:

$$v \quad \leq \quad 15.5\,\mathrm{m/s} \qquad \text{| short pipe} \tag{7}$$

$$v \quad \leq \quad 8.0\,\mathrm{m/s} \qquad \text{| long pipe} \tag{8}$$

To determine suitable hose diameters, the continuity equation must be applied in conjunction with the velocity constraints and the required mass flow. This mass flow is derived from the aircraft's energy demand, as listed in Table 1, and converted into LH2 mass using the hydrogen's mass-specific energy (see Section 2.2) along with an assumed propulsion efficiency (e.g., 50 % for a fuel cell system). The LH2 requirement for the representative of GA aircraft (e.g., Cessna 208) amounts to approximately 246 kg. For light manned aircraft (e.g., e-Genius), the corresponding LH2 requirement is about 4 kg, and for UAVs, less than 0.1 kg. At these low quantities, conventional cryogenic transfer mechanisms become oversized and inefficient, underscoring the need for micro-scale LH2 refueling systems tailored to autonomous, small-scale applications. The results of the LH2 refueling system scaling for these aircraft classes are presented and discussed in Section 4.1.

3.3 Ground Energy Supply for Batteries

Ground-based electrical energy supply strategies, such as charging or battery swapping, require thorough evaluation to ensure compatibility with aircraft turnaround requirements. Battery accessibility within the airframe becomes a critical factor, particularly in scenarios involving battery swaps or future upgrades, as higher mass-specific energy battery technologies become available [19]. Despite these potential use cases, onboard battery charging is typically favored [19], primarily due to its lower handling complexity and reduced personnel requirements [70].

DOI: 10.13009/EUCASS2025-453

Fixed battery integration further offers advantages for commercial aircraft, including reduced structural mass and improved safety through permanent internal connections [70]. Consequently, fast charging is often prioritized over battery swapping, despite the high infrastructure costs associated with grid integration and the challenges of mitigating peak electrical loads [70]. High-power charging introduces several technical challenges, including the need for advanced Thermal Management Systems (TMS), strategies to mitigate battery degradation, and reinforcement of airport electrical infrastructure to accommodate elevated peak loads [17]. Fast charging is well-suited for gate-based implementation, as it aligns with existing energy supply infrastructure and avoids the logistical complexities of mobile truck-based operations, which remain common in conventional refueling systems [19, 70].

Battery swapping provides an alternative to onboard charging by enabling grid-friendly recharging at lower, constant rates [17]. In the automotive sector, battery swapping has been demonstrated as a viable alternative to conventional charging [71–73]. Battery swap stations typically allow electric vehicles to autonomously enter a designated bay, where an automated system exchanges the depleted battery with a fully charged one before the car exits the station [71]. Depending on the vehicle architecture, battery access can be facilitated from the side, rear, top, or underside, with some configurations enabling side-mounted swaps [71]. Swap durations vary based on vehicle class and battery size. For instance, the automotive manufacturer NIO reports complete battery swaps for electric vehicles in approximately 5 minutes [73], while electric taxis can be serviced in 90 seconds [72]. Heavy-duty trucks, carrying battery packs weighing up to 2500 kg, typically require around 8 minutes for a full exchange [72].

Comparative studies of turnaround procedures underscore the operational trade-offs between battery charging and swapping [18]. Swapping may offer shorter TATs and enables a flatter power profile by allowing batteries to be recharged offboard at lower, more constant grid loads [17]. However, it requires substantial mechanical infrastructure, specialized handling equipment, and increased personnel involvement due to safety inspection protocols [70]. An additional benefit of swapping is improved thermal management, as removed batteries can be cooled outside the aircraft during recharging between flights [17]. Given these considerations, the following sections examine both battery charging and battery swapping as viable methods for ground energy supply in hybrid-electric aircraft operations.

3.3.1 Fast Charging

In the present study, battery charging is modeled as a Direct Current (DC) fast-charging process, which is essential for hybrid-electric aircraft due to their high power demand and the impracticality of carrying bulky onboard conversion electronics [74]. Unlike Alternating Current (AC) systems, DC charging shifts most power conversion and control components offboard, enabling higher power transfer without significantly increasing aircraft weight [74].

The standard charging protocol for lithium-ion batteries is Constant Current-Constant Voltage (CC-CV), as it offers a favorable balance between charging speed, efficiency, and battery longevity [75–78]. Widely adopted in electric mobility, CC-CV is valued for its simplicity and its ability to manage thermal and electrochemical stresses during high-power charging [77, 78]. During the CC phase, the battery is charged at a fixed current until a predetermined voltage limit is reached, typically around SoC = 80 % [75, 77]. This is followed by the CV phase, where the voltage is held constant and the current tapers off gradually to prevent overcharging and mitigate degradation risks [75, 77]. This gradual transition is crucial for preserving battery cycle life, making the CC-CV approach a dual strategy for both performance and longevity [75]. However, charging from 80 % to 100 % SoC under the CV phase can nearly double the total charging time [75]. Moreover, applying high charging currents beyond 80 % SoC can accelerate degradation and reduce the number of usable cycles [79, 80].

In this study, degradation effects are neglected for simplification purposes. Battery charging time depends on the assumed C-rate, with duration modeled as the inverse of the C-rate and approximated as linear. As a result, the charging time t_{charging} is calculated based on CC charging using a fixed C-rate, as described in Equation 3:

$$t_{\text{charging}} = \frac{\text{SoC}_{\text{max}} - \text{SoC}_{\text{min}}}{C_{\text{rate}}} \tag{9}$$

This simplification impacts both the estimated charging time and the projected battery degradation. Therefore, the implications of charging on aircraft-level design are further examined in Section 4.3.

Due to the substantial energy requirements of commercial aircraft, the charging infrastructure must support high voltages to reduce cable mass and associated thermal losses [74, 81]. For example, charging at 350 kW is feasible at 800 V [81]. However, higher voltages (up to 1500 V) are necessary to enable megawatt-level power transfer while keeping current levels and cable dimensions manageable [74, 81]. At these power levels, liquid-cooled cables offer a viable solution to mitigate thermal stress and reduce cable cross-sections [74, 81].

For details on various automotive charging plug standards, refer to Tu et al. [81] and Liang et al. [77]. The methodology adopted in this study incorporates compatibility with emerging standards, particularly the Megawatt Charging System (MCS), including the corresponding high-power charging plug [74, 77]. MCS targets maximum power ratings of up to 3750 kW, with theoretical extensions to 4500 kW at 1500 V and 3000 A [74, 77].

DOI: 10.13009/EUCASS2025-453

These systems also support galvanic isolation through the use of isolated DC/DC converters, which is essential to ensure operational safety and battery protection, as the battery must remain electrically isolated from ground at all times [81]. Alternatively, conductive DC charging interfaces may also be considered, aligning with current industry practices and ensuring compatibility with anticipated infrastructure developments [77, 81].

3.3.2 Swapping

Battery swapping introduces a range of regulatory and procedural challenges that must be addressed to enable its integration into commercial aircraft operations. This section outlines the key legal, operational, and safety considerations relevant to battery swapping in hybrid-electric aviation. Battery swapping processes also differ significantly in duration, required equipment, and procedural complexity across aircraft classes.

Maintenance Classification and Personnel Requirements: According to 14 CFR Part 43 [82], battery replacement qualifies as preventive maintenance only if it involves non-complex procedures. For battery swapping to remain within this category, battery modules must be easily accessible and installable. Otherwise, swaps could be reclassified as base maintenance, which would increase personnel and documentation requirements and complicate turnaround integration. For aircraft with more than 20 passengers or payloads over 2722 kg (14 CFR Part 125 [83]), maintenance actions, including battery swaps, must be certified by two qualified individuals. In contrast, smaller aircraft allow greater flexibility, with approval potentially granted by a single technician or even the pilot (14 CFR Part 43.3 [82]). If battery swaps are defined as preventive maintenance, trained personnel could perform the task under the supervision of a licensed mechanic.

Documentation and Operational Feasibility: Per 14 CFR Parts 43.11 [82] and 91.417 [84], all maintenance actions must be documented, including signatures and certification details. While this is manageable for standard checks, it presents a logistical challenge for battery swaps during short TATs. A simplified log entry retained until the next swap may suffice, but this must be coordinated with the aircraft's return-to-service clearance and pilot briefing (14 CFR Part 125.73 [83]).

Occupational and System Safety: Manual handling of batteries must comply with occupational safety standards. Recommended limit is about 25 kg depending on lifting frequency [77, 85, 86]. Exceeding these thresholds necessitates the use of mechanical aids or reduced handling frequency. Consequently, the mass of the battery module must be taken into account in system design. Battery swapping also presents safety advantages. Unlike fast charging, which may stress TMS, swapped batteries can be cooled and inspected offline. Damaged batteries can be isolated and analyzed without delaying flight operations.

To assess the operational feasibility of battery swapping in aviation, the procedures of battery disconnection, unloading, loading, connection, and verification are systematically analyzed across four representative aircraft classes. Time estimates for battery loading and unloading are derived from container cargo handling in commercial aviation, typically requiring approximately 1.5 min for each. Ground vehicle positioning and door opening are assumed to take 2 min, while equipment removal and door closing add another 1.5 min.

Depending on the airport or airfield infrastructure and, consequently, the aircraft class, the durations of these steps are adapted to reflect varying degrees of automation, ranging from manual handling to semi-automated operations using ground support vehicles, such as airport container transporters or single-platform container loaders. The operational characteristics of such vehicles are detailed in Mensen [87]. Additionally, platform lifting is estimated to require approximately 1 min to raise a load by 2 m [88]. Battery disconnection and reconnection are assumed to follow procedures similar to those used in high-power charging, such as with the MCS plug.

3.4 Discussion of Simultaneous Operations

The feasibility of simultaneous operations – specifically refueling in parallel with battery charging or battery swapping (and passengers onboard) – offers a promising pathway to minimize TATs without compromising safety. According to current safety protocols, such as those outlined in explosion protection regulations [89, 90], the presence of a dangerous explosive atmosphere is the primary determinant of the necessity for ignition protection zones. In the absence of such an atmosphere – ensured through primary explosion protection via permanently technically tight systems and positive gauge pressures – no additional explosion protection measures are required, even close to fueling zones [52].

For Jet A-1 and LH2, refueling with passengers onboard is permissible under these conditions, provided that system integrity is continuously monitored and failsafe mechanisms are in place. By extension, battery charging or swapping operations may also be conducted in parallel with refueling, as long as they adhere to comparable safety protocols – typically requiring a minimum separation radius of 3 m for ground servicing activities during refueling operations [91]. For regional aircraft with an approximate fuselage length of 30 m, such spatial separation is feasible within the standard constraints of airport ramp layouts.

DOI: 10.13009/EUCASS2025-453

Furthermore, in analogy to automotive standards, battery-related operations – such as charging and even swapping – can be carried out while occupants are onboard. Battery swapping, in particular, enhances safety by allowing damaged or degraded modules to be isolated and replaced. While the co-location of high-voltage charging or battery swap systems with fuel systems may raise concerns, such operations can be performed safely if established handling protocols and standards are adhered to. Future airport layouts should incorporate zoning provisions for simultaneous operations, ensuring that safety distances and infrastructure (e.g., grounding, shielding) must comply with the ATEX directives [92, 93] and other applicable regulations. These developments could enable integrated turnaround procedures that may uphold regulatory compliance while significantly improving aircraft competitiveness.

3.5 Charging Implications in Preliminary Aircraft Design

This section outlines the workflow for evaluating the implications of charging interactions during the preliminary aircraft design process. The workflow, iterative sizing loop, and the hybrid-electric propulsion architecture are implemented in Python 3.9, adapted from Mangold et al. [94, 95] as part of an enhanced version of the SUAVE framework. SUAVE [96, 97] is an open-source environment for preliminary aircraft design.

For the analysis of charging implications, the Serial-Parallel Partial Hybrid (SPPH) propulsion architecture is adopted. This hybrid-electric configuration utilizes two energy carriers and has been identified as a promising concept [94, 95, 98–100]. The distribution of energy usage between the carriers is governed by an Energy Management Strategy (EMS), which defines the proportion of battery usage across different mission segments. The EMS essentially controls the throttle of the electric motors, thereby determining the extent to which the battery contributes to propulsion. Three EMS variants are considered: EMS1, where the battery powers the electric motor in all flight segments except descent; EMS2, which excludes battery use during cruise and descent; and EMS3, where the battery is only used during the climb and reserve climb segments [94, 95].

Charging implications primarily affect battery sizing. Battery sizing is typically guided by the Ragone diagram, which relates mass-specific energy to mass-specific power. The selected battery technology must satisfy both the mission-specific energy demand and peak power requirements, ensuring compatibility with the mass-specific performance characteristics indicated by the Ragone diagram.

In addition to the discharge profile, this study introduces charging requirements as a novel constraint in battery system sizing. Specifically, a required charging C-rate is defined, which determines the necessary charging power based on the total mission energy. The maximum of the discharge power and the power of charging power required is used as the input for battery sizing. This approach introduces a snowball effect: different EMS and C-rate requirements result in varying battery sizes, which subsequently impact aircraft mass and performance. The iterative design loop converges to distinct aircraft configurations depending on these interdependencies. The impact of varying the charging C-rate from 0 (i.e., no charging constraint) to $3\,\mathrm{h}^{-1}$ (i.e., 20 min charging) across different EMSs is presented in Section 4.3.

4. Results

In this section, the results of the analysis of dual-energy carrier aircraft, focusing on refueling and turnaround operations, are presented. The findings include the scaling of LH2 refueling systems for different aircraft classes. Additionally, the procedures and time requirements, as well as boundary conditions for both onboard battery charging and battery swapping, are outlined and discussed. Furthermore, implications for aircraft design and the interactions associated with onboard battery charging are analyzed. Finally, the results are translated into corresponding airport infrastructure requirements, which must be fulfilled to enable such turnaround operations and ensure the competitiveness of these aircraft.

4.1 Refueling of Liquid Hydrogen

To satisfy the energy demands of hydrogen-powered aircraft within typical turnaround constraints, a class-specific scaling of refueling requirements is conducted. For GA aircraft, a conventional turnaround time of 19 minutes is assumed [23]. Accounting for 6 minutes of connection, disconnection, and chill-down—estimated similarly to larger aircraft due to comparable ground handling constraints – yields a net refueling window of 13 minutes. For a Cessna 208-like aircraft requiring approximately 426 kg of LH2 (see Section 3.2), this translates to an average mass flow rate of roughly 0.35 kg/s. Applying the continuity equation alongside the empirical constraints in Equations 6 and 7 results in an optimal hose inner diameter of approximately 20.2 mm. Although significantly smaller than those used for commercial aircraft (152.4 mm), this dimension enables adequate flow rates while maintaining a suitable flow regime.

To simplify logistics and reduce cost through standardization – particularly given that GA and light manned aircraft often operate from the same airfields. It is assumed that both aircraft types use a shared refueling disconnect.

DOI: 10.13009/EUCASS2025-453

Consequently, a standard hose diameter of 20.2 mm, with a maximum allowable mass flow of 0.35 kg/s, is proposed for these categories. For light manned aircraft, although the LH2 requirement is significantly lower (e.g., 4.0 kg), the shared hose diameter may be oversized. However, the benefits of standardization justify this simplification. The maximum mass flow is excessive for this class, but it could be reduced by either lowering the system pressure (in a pressure-fed setup) or adjusting the pump speed (in a pump-fed refueling system).

In contrast, for small UAVs such as delivery drones, the required LH2 mass per mission is extremely low (e.g., < 0.1 kg). Considering the high utilization rates and the potential deployment of thousands of such vehicles, custom-designed refueling interfaces are not only feasible but also necessary and practical. Assuming full automation and rapid connection/disconnection (aligned with UAV battery swapping benchmarks, see Section 4.2.2), a net LH2 refueling time of 30 s is assumed for competitiveness, totally 1 min. For a 0.1 kg demand, this results in a required mass flow of 0.0033 kg/s, which corresponds to a hose inner diameter of approximately 2.0 mm. Table 2 summarizes the results of this scaling analysis.

Table 2: Scaled LH2 refueling parameters for different aircraft classes. The table presents LH2 mass, target refueling time, resulting mass flow, and hose inner diameter for GA and UAVs. Values are derived from mission-specific energy demands and empirical flow constraints, illustrating the need for size-appropriate refueling systems.

Aircraft Class	**LH2 Mass** in kg	**Refueling Time** in min	**Mass Flow** in kg/s	**Inner Hose Diameter** in mm
General Aviation	246	13	0.3500	20.2
UAV	0.1	0.5	0.0033	2.0

However, such a small inner diameter may pose challenges for current manufacturing techniques and mechanical robustness. Therefore, a more practical minimum inner diameter of 5 mm may be chosen instead. While this increases the cross-sectional area, it allows the same mass flow to be achieved at a significantly lower velocity, aligning also with the constraints in Section 3.2. Furthermore, due to the use of clean-break disconnects, helium purging is not required. At small or decentralized airfields, recovery lines for vaporized hydrogen may also be impractical due to the cost of collecting and liquefaction infrastructure. In such cases, passive venting systems, such as chimneys, may be employed. Alternatively, using subcooled LH2 or designing tanks with slightly higher allowable pressures could reduce or eliminate the need to vent hydrogen entirely.

Ultimately, while commercial LH2 infrastructure provides a valuable foundation, its direct application to smaller aircraft classes is not viable. A dimensionless, mission-specific scaling approach is essential to enable safe, efficient, and technically appropriate LH2 refueling across the full spectrum of emerging hydrogen-powered aviation platforms.

4.2 Battery Handling for Turnaround Operations

Efficient battery handling is a critical enabler for hybrid-electric aircraft to remain operationally competitive. This section compares two key strategies – onboard charging and battery swapping – with respect to their technical feasibility, process duration, and compatibility with aircraft turnaround requirements. Charging durations are governed primarily by the C-rate, while swapping depends on standardized battery design and ground handling logistics.

4.2.1 Onboard Charging

The charging time of a battery is directly governed by the applied C-rate, following an inverse proportionality as described in Equation 9. Assuming CC charging and neglecting degradation effects, the charging duration scales linearly with the SoC window and inversely with the C-rate. For example, a C-rate of $1\,\mathrm{h}^{-1}$ results in a charging time of 60 minutes, whereas a C-rate of $2\,\mathrm{h}^{-1}$ enables charging within 30 minutes. This relationship underscores the critical importance of high C-rates in achieving turnaround-compatible charging durations.

As noted in Section 3.1, turnaround operations are expected to be completed within approximately 30 minutes. The time required to connect and disconnect the charging interface – such as the MCS discussed in Section 3.3.1 – is comparable to existing ground power unit procedures. A duration of 2.5 minutes for each process is therefore adopted, consistent with typical values for refueling hose operations [36]. Accounting for these interface handling times, the net available charging time is reduced to approximately 25 minutes. According to Equation 9, this necessitates a minimum C-rate of approximately $2.4\,\mathrm{h}^{-1}$ for a full charge. When considering a typical SoC window of 10 to 80 %, a slightly lower C-rate of around $2.1\,\mathrm{h}^{-1}$ is sufficient.

DOI: 10.13009/EUCASS2025-453

However, practical limits on the achievable C-rate arise from constraints related to thermal management and airport power infrastructure. These challenges are further analyzed in the context of aircraft-level integration in Section 4.3 and airport infrastructure requirements in Section 4.4.

4.2.2 Swapping

To ensure the economic feasibility of battery swapping, battery modules should be designed as standardized, modular units compatible with a wide range of aircraft types. These modules are composed of individual battery cells and are combined to form a complete battery pack. Without such standardization, the specialization of individual airfields in specific battery types would significantly reduce operational flexibility and limit cross-location compatibility. Standardization should therefore extend to offboard charging infrastructure, logistics, and installation procedures. Accordingly, battery modules should be universal, lightweight, and appropriately dimensioned. They must support quick and straightforward mounting, with a modular architecture that enables the assembly of larger battery packs as required. Ideally, the fully assembled battery system should interface with the aircraft via a single connection point.

As outlined in Section 3.3.2, and by occupational safety guidelines, the handling mass of each battery module does not exceed 25 kg, ensuring suitability for manual handling. To further minimize the need for additional protective measures, each module is limited to a nominal voltage of 60 V DC. This threshold complies with the safety extra-low voltage limits defined in DIN VDE 0100-410 [101], which state that no supplementary protection against direct contact is required below 60 V DC in dry environments. Furthermore, IEC 61140 [102] defines that equipment relying solely on voltage limitation for basic protection (and lacking fault protection) may operate up to 120 V DC. Nonetheless, this study maintains the conservative 60 V DC limit to ensure maximum handling safety. Battery systems based on such modules can therefore be safely handled without the need for complex insulation or enclosure designs [103], simplifying both logistics and ground operations.

For UAVs, a fully automated battery swapping process is assumed. This assumption is based on the work of Liu et al. [104], who demonstrated a swap duration of 49 s. Including a small buffer, the total time estimated for battery swapping is 1 min.

For light manned aircraft, battery swapping requires the presence of a certified mechanic. The mechanic is responsible for safely disconnecting the battery, connecting the replacement unit, verifying correct installation, and issuing written clearance to the pilot. Due to the compact and lightweight design of such aircraft, it is assumed that minimal ground support equipment is required and that most procedures are performed manually, i.e., by a person. The following time allocations are considered for each step: battery disconnection is estimated to take 2 minutes; unloading and reloading of each battery module using a mobile lifting table requires 1 minute per module; an additional 1 minute is included as a buffer for the loading process. The battery connection is expected to take approximately 2 minutes, with a further 1 minute allocated as a buffer for this step. Final verification and pilot clearance are assumed to take 2 minutes. Assuming twelve battery modules (i.e., a total battery mass of 290 kg divided into twelve 25 kg modules), the overall battery swap procedure results in a total swapping time of approximately 20 minutes.

In the scenario for GA aircraft, the fully charged battery must first be transported to the aircraft's parking position using an airport dolly designed for unit load devices. Due to the limited availability of commercial ground support equipment at smaller regional airfields, a forklift is assumed to transfer the battery onto a lifting platform. It is further assumed that the battery modules are pre-assembled into a single unit at the offboard charging station, implying that only one loading operation is required. Considering these operational requirements, the procedure is broken down as follows: battery disconnection is estimated to take 2 minutes; unloading the battery requires 3 minutes; loading the replacement battery takes an additional 3 minutes; electrical connection is assumed to take 2 minutes; system verification is expected to require 4 minutes; and a buffer time of 4 minutes is included to account for minor delays or handling variations. This results in a total battery swapping duration of approximately 18 minutes. Justin et al. [17] reported a total swap time of about 5 minutes for comparable aircraft, although this figure appears optimistic given the practical constraints outlined above.

For regional aircraft, the fully charged battery is transported to the aircraft using an airport container transporter and positioned with a single-platform container loader. Similar to the GA scenario, the battery consists of multiple modules that are pre-assembled into a single unit at the offboard charging station. As a result, the increased battery mass does not inherently extend the battery swapping time, since modular handling is avoided. The estimated procedure is as follows: battery disconnection is assumed to take 2 minutes; unloading the depleted battery from the aircraft requires approximately 5 minutes; loading the replacement battery takes an additional 5 minutes; battery connection is expected to take 2 minutes; system verification is estimated at 4 minutes; and a buffer of 2 minutes is included to account for operational uncertainties. Compared to GA aircraft, an additional 1 minute is allocated for loading and unloading due to the slower operating speed of the pallet transporter relative to the forklift used in the GA case. This results in a total estimated battery swapping duration of 18 minutes.

DOI: 10.13009/EUCASS2025-453

In summary, battery swapping appears to be operationally feasible within the aircraft turnaround process, particularly if it can be performed in parallel with other ground handling procedures. Across all reference aircraft, the total battery swapping time remains under 20 min, aligning well with typical turnaround durations. Specifically for regional aircraft, the battery swap requires a TAT that is 3 min longer than the conventional process (see Section 2.1). While this marginal increase may impact aircraft utilization and revenue, it is offset by assumptions of optimized, automated swapping and streamlined verification procedures. These findings indicate that, with well-coordinated ground operations, battery swapping can serve as a viable alternative to onboard charging without significantly extending TATs. However, its economic implications should be evaluated as part of a broader cost-benefit analysis of hybrid-electric aircraft operations.

4.3 Battery Charging Influence on Aircraft Performance

This section presents the impact of battery charging requirements on preliminary aircraft design, using the regional aircraft ATR 42 (MTOM = 18.600 kg [69]) as a reference hybrid-electric platform. As outlined in Section 3.5, the methodology entails varying the charging C-rate across different EMSs, while keeping the Top-Level Aircraft Requirements (TLAR) [21] and a fixed design mission range of 400 km constant. The outcomes of this parametric analysis are summarized in Table 3. All cases assume a power hybridization factor of $H_P = 0.2$. The usable SoC window is defined from $SoC_{min} = 10\,\%$ to $SoC_{max} = 80\,\%$, which also applies to the discharge flight profile.

Table 3: Impact of charging C-rate and EMS on aircraft performance for a hybrid-electric regional aircraft. All aircraft assume a constant hybridization factor of $H_P = 0.2$ and a mission range of 400 km. The usable SoC window ranges from $SoC_{min} = 10\,\%$ to $SoC_{max} = 80\,\%$. The sizing C-rate is highlighted in bold.

EMS	**Char. C-rate** in h^{-1}	**MTOM** in kg	**Trip Fuel** in kg	**Battery** in kg	**Spec. Energy E_S** in Wh/kg	**Spec. Power P_S** in W/kg	**Dis. C-rate** in h^{-1}
1	0	21699	356	3058	546	254	**0.47**
	1	22390	365	3490	494	494	0.47
	2	23145	374	3964	447	893	0.47
	3	23603	381	4278	419	1258	0.47
2	0	20893	419	2367	525	331	**0.63**
	1	21165	423	2544	494	494	0.63
	2	21653	430	2864	447	893	0.63
	3	22126	440	3130	419	1258	0.63
3	0,1	18791	389	844	449	863	**1.92**
	2	18801	389	849	447	893	1.92
	3	18892	390	909	419	1258	1.92

The discharge C-rates in Table 3 are relatively low for EMS1 and EMS2, as the battery is used throughout most flight segments, leading to high mission energy demand. In the sizing approach, both the peak discharge and charging power are considered, significantly affecting performance indicators such as MTOM, trip fuel, and battery mass. For example, in EMS1, increasing the charging C-rate from 0 to $3\,h^{-1}$ results in a rise of approximately 9 % in MTOM, 4 % in fuel consumption, and 40 % in battery mass.

Notably, the relative importance of mass-specific energy and mass-specific power shifts as the charging C-rate increases. For EMS1 and EMS2 with a charging C-rate of 0, sizing is primarily driven by mission energy demand (i.e., E_S). However, as the charging C-rate increases, specific power becomes the dominant constraint, because the increasing P_S indicates that the battery sizing attempts to make a lighter battery, neglecting the E_S. However, with increasing charging C-rates, specific power becomes the dominant constraint. This is because the rising P_S reflects a design trend toward lighter battery packs, with less emphasis on E_S. EMS3 differs in that the battery is used in fewer flight segments, resulting in a higher discharge C-rate of approximately $1.9\,h^{-1}$. Consequently, aircraft performance remains largely unaffected by the charging C-rate until it exceeds the discharge rate (i.e., at C-rate $3\,h^{-1}$), after which only minor performance changes occur.

Feeding back these findings into aircraft utilization and TAT analysis, which demands a charging C-rate of $2.1\,h^{-1}$ for competitive operation (see Section 3.1), the implications become more pronounced. The battery and associated subsystems, including aircraft metrics, would then be sized primarily for the charging requirement rather than the energy demand of the mission. This shift can significantly affect fuel consumption and emissions, which increase by up to 4 %. Such an outcome could minimize the environmental benefits of hybrid-electric propulsion.

DOI: 10.13009/EUCASS2025-453

Conversely, if the charging requirement is not considered, the battery must be charged at a C-rate that does not exceed its maximum discharge C-rate. This omission leads to excessive charging times (see Equation 9) – approximately 90 min for EMS1 and 67 min for EMS2. As shown in the turnaround analysis in Section 2.1, such prolonged charging durations would reduce aircraft utilization to around 50 %, posing a significant challenge to the economic viability of hybrid-electric aircraft. On the other hand, incorporating the charging requirement increases fuel consumption and emissions, thereby reducing environmental competitiveness. However, it enables aircraft operations with conventional utilization levels, preserving operational feasibility.

Heat Load and Thermal Management System

As previously discussed, the charging constraint not only influences overall aircraft performance but also imposes additional demands on the TMS. Specifically, higher charging powers result in increased heat generation ($\dot{Q}_{\text{bat,heat}}$) due to resistive losses, necessitating the use of larger or more efficient TMS components to maintain safe operating conditions.

Table 4 illustrates the estimated thermal impact of varying charging C-rates for the EMS1 battery system, assuming a battery voltage of 1000 V and an internal resistance of 50 mΩ. The discharge C-rate of $0.47\,\text{h}^{-1}$, representative of typical flight mission demands with varying battery energy levels (see Table 3), serves as the baseline for sizing the TMS. As the charging C-rate increases, both the charging power and associated heat generation rise significantly – following an approximately quadratic relationship, as described by Equation 5.

Table 4: Estimated charging power and thermal load for varying charging C-rates in the EMS1 battery system. Heat generation is calculated for a battery voltage of 1000 V and internal resistance of 50 mΩ, using a discharge C-rate of $0.47\,\text{h}^{-1}$ as the thermal management system baseline.

Charg. C-rate in h^{-1}	**Charg. Power** in kW	**Charg. Heat** $\dot{Q}_{\text{heat,charg}}$ in kW	**Heat Ratio** $\dot{Q}_{\text{heat,charg}}/\dot{Q}_{\text{charg,discharg}}$ in −
0.47	777	31	1.0
1.0	1724	149	4.5
2.0	3540	628	18.1
3.0	5382	1446	40.7

While higher C-rates facilitate shorter charging durations and enable faster turnarounds, they also introduce substantial thermal loads. At a C-rate of $3.0\,\text{h}^{-1}$, the heat generated during charging reaches 1446 kW – more than 40 times greater than the heat load at the baseline discharge C-rate of $0.47\,\text{h}^{-1}$. This corresponds to the expected quadratic scaling: $(3/0.47)^2 = 40.7$. Managing such elevated thermal loads with onboard systems alone would necessitate significantly oversized TMS components, which would adversely affect the aircraft's mass, volume, and energy efficiency.

This scaling behavior highlights a fundamental trade-off in electric aircraft design – while rapid charging enhances operational efficiency, it simultaneously imposes disproportionate thermal burdens. As onboard cooling becomes impractical at elevated C-rates, the deployment of offboard thermal management infrastructure becomes essential to ensure charging operations. Section 4.4.1 provides further detail on these offboard cooling strategies and their integration into airport ground support systems.

4.4 Airport Infrastructure Requirements

The integration of dual-energy carrier aircraft into commercial aviation introduces substantial infrastructure demands at airports. For SAF, as described in Section 2.2.1, no significant deviations from existing airport infrastructure are anticipated. In contrast, LH2 infrastructure requires additional space and components – such as storage tanks, new pipeline systems, or mobile refueling units – depending on airport size and techno-economic considerations, as discussed by Hoelzen et al. [49–51] and Mangold et al. [40, 52]. The integration of battery-electric or hybrid-electric propulsion imposes particularly high demands on airport infrastructure, especially in the context of high-power charging and battery swapping. Each strategy presents distinct requirements for the airport infrastructure, which will be evaluated in detail in this section.

DOI: 10.13009/EUCASS2025-453

4.4.1 High-Power Charging Influence

To support fast charging, airports will require substantial upgrades to their electrical infrastructure. The energy demand associated with megawatt-scale charging necessitates reinforced grid connections and, in many cases, the integration of intermediate energy storage systems to buffer peak loads and mitigate stress on the local power supply network [70]. Additionally, charging stations must be installed at or near every gate to enable rapid energy transfer within short TATs. While fixed ground-based charging points are preferred for grid integration, operational reliability, and safety, mobile charging vehicles, analogous to conventional fuel trucks, may offer flexible solutions during early deployment phases or at secondary airfields with limited infrastructure [19].

The total electrical power requirement during high-rate charging is governed not only by the battery's energy input but also by resistive losses. As shown in Table 4, charging at elevated C-rates requires approximately 5.4 MW of electrical power for battery charging alone. When accounting for associated resistive losses (up to 1.4 MW), the total instantaneous power demand per aircraft can rise to approximately 6.8 MW. This peak load must be considered in airport electrical infrastructure planning, particularly if multiple aircraft are to be charged simultaneously. The currently available MCS is rated for charging powers up to 4500 kW (see Section 3.3.1). Therefore, regional aircraft exceeding this threshold would require the development of enhanced charging systems tailored to their specific power requirements.

High-power charging also imposes thermal management requirements that far exceed those encountered during standard flight operations. As discussed in Section 4.3, the onboard TMS is typically sized to handle the heat loads generated during battery discharge. However, the substantially higher heat fluxes associated with fast charging necessitate enhanced cooling strategies. If not adequately dissipated, this heat can accelerate battery degradation and potentially initiate safety-critical events such as thermal runaway [105]. To mitigate these risks, the implementation of advanced external cooling solutions must be investigated [105].

Given the magnitude of thermal loads during high-C-rate charging, offboard TMSs may be required, particularly when onboard cooling capacity is insufficient. These systems could be integrated into charging trucks or fixed ground infrastructure [70]. Ideally, a multi-functional connector would enable both electrical and thermal coupling between the aircraft and the ground system. For example, Joby Aviation [106] has developed a unified power and cooling interface to support this type of integrated operation. Therefore, future ground infrastructure must not only support high-power electrical transfer but also facilitate efficient thermal exchange.

4.4.2 Battery Swapping Influence

Battery swapping represents a promising alternative to onboard charging by decoupling energy supply from the aircraft's operational turnaround, allowing batteries to be recharged offboard under optimized, low-stress conditions. However, the successful implementation of this strategy demands significant adaptations to airport infrastructure. A fundamental prerequisite is the standardization of battery modules across various aircraft types and manufacturers. Without harmonized dimensions, voltage specifications, and interface protocols, each aircraft would require customized battery packs, leading to increased logistical complexity, higher inventory requirements, and limited interoperability across fleets.

Additionally, dedicated storage facilities are required to house the battery modules. These hubs must support controlled environmental conditions, fire suppression systems, and scalable layout designs to handle varying throughput demands. Charging should occur centrally at these hubs using available grid capacity, ideally during off-peak hours to minimize peak loads and reduce operational costs.

To enable fast and safe battery swapping, specialized ground support vehicles must be developed and certified. These systems must ensure precise positioning, low-vibration handling, and compliance with stringent aviation safety standards. They should also facilitate (semi-)automated operation to reduce the workload on airport personnel and ensure consistent procedural safety. The handling mass and volume of battery packs – particularly for regional aircraft – demand robust lifting platforms and mechanical coupling mechanisms that allow rapid but secure detachment and reattachment.

From a broader perspective, airport infrastructure must be reconfigured to integrate these systems efficiently. This includes designated battery handling zones, logistic pathways that do not interfere with passenger operations, and coordinated processes with aircraft servicing schedules. Additionally, the infrastructure should be scalable and modular to accommodate future growth in electric aircraft fleets without imposing excessive manpower or operational burdens on airport operators [19].

While the mechanical integration and logistical demands of battery swapping are more complex than those of conventional charging, this approach offers substantial operational advantages – particularly for high-utilization aircraft or in airports lacking megawatt-scale electrical infrastructure. When properly implemented, battery swapping can significantly enhance turnaround efficiency while supporting long-term energy and emissions targets in aviation.

DOI: 10.13009/EUCASS2025-453

5. Conclusion

This study investigates the operational, economic, and infrastructural implications of integrating dual-energy carrier systems – combining Sustainable Aviation Fuels (SAFs) or Liquid Hydrogen (LH2) with onboard battery systems – into aircraft turnaround operations. The findings underscore the necessity of simultaneously optimizing aircraft design, turnaround procedures, and airport infrastructure to ensure competitive turnaround times and economic viability.

Battery handling emerges as a key operational driver: high-power onboard charging at a C-rate of approximately $2.4\,\mathrm{h}^{-1}$ supports compliance with standard turnaround windows but introduces substantial demands on thermal management and electrical infrastructure. Alternatively, (semi-)automated battery swapping proves feasible within 20 minutes across aircraft classes, offering advantages such as reduced peak electrical loads and the ability to shift charging offboard, easing thermal requirements. However, this strategy requires standardized battery modules, automated handling systems, and coordinated logistics.

For LH2, the refueling procedure and ground vehicle connection are specifically scaled for smaller aircraft classes, reflecting lower volumetric and flow requirements. Corresponding interfaces and procedures can thus be dimensioned appropriately to reduce spatial and technical complexity.

The methodology developed herein is designed to be flexible and scalable, enabling application across a wide range of aircraft sizes. Ultimately, the successful integration of dual-energy carriers depends on a holistic design approach – one that aligns operational strategies, aircraft design, and ground operations to ensure sustainable and economically viable next-generation aviation.

References

[1] European Commission and Directorate-General for Research and Innovation. *Fly the Green Deal – Europe's vision for sustainable aviation*. Publications Office of the European Union, LU, 2022.

[2] European Commission. The European Green Deal COM(2019) 640. Available online: https://eur-lex.europa.eu/resource.html?uri=cellar:b828d165-1c22-11ea-8c1f-01aa75ed71a1.0002.02/DOC_1&format=PDF (accessed on 18 July 2024).

[3] European Commission. Directorate General for Research and Innovation. and European Commission. Directorate General for Mobility and Transport. *Flightpath 2050 :Europe's Vision for Aviation : Maintaining Global Leadership and Serving Society's Needs.* Publications Office, LU, 2011.

[4] Ingmar Geiß. *Sizing of the Series Hybrid-Electric Propulsion System of General Aviation Aircraft*. PhD thesis, University of Stuttgart, 2020.

[5] Jonas Mangold, Felix Brenner, Nicolas Moebs, and Andreas Strohmayer. Aircraft Design Implications of Alternative Fuels for Future Hybrid-Electric Regional Aircraft Configurations. In *Proceedings of the 9th European Conference for Aerospace Sciences. Lille, France, 27 June - 1 July, 2022*, 2022.

[6] I. Geiß and R. Voit-Nitschmann. Sizing of the energy storage system of hybrid-electric aircraft in general aviation. *CEAS Aeronautical Journal*, 8(1):53–65, March 2017.

[7] Martin Hepperle. Electric Flight - Potential and Limitations. In *Energy Efficient Technologies and Concepts of Operation*, Lisbon, October 2012.

[8] Tianhong Jiang, Yaolong Liu, Yao Zheng, and Ali Elham. Investigating the potential of parallel hybrid-electric retrofit of narrow-body airliner for emission reduction. *Proceedings of the Institution of Mechanical Engineers, Part G: Journal of Aerospace Engineering*, 237(16):3753–3768, November 2023.

[9] Valerio Marciello, Mario Di Stasio, Manuela Ruocco, Vittorio Trifari, Fabrizio Nicolosi, Markus Meindl, Bruno Lemoine, and Priscilla Caliandro. Design exploration for sustainable regional hybrid-electric aircraft: A study based on technology forecasts. *Aerospace*, 10(2):165, February 2023.

[10] Francesco Orefice, Fabrizio Nicolosi, Salvatore Corcione, and Pierluigi Della Vecchia. Hybridization and mission analysis of a regional turboprop. In *AIAA AVIATION 2021 FORUM*. American Institute of Aeronautics and Astronautics, July 2021.

[11] Chrysoula L. Pastra, Gokcin Cinar, and Dimitri N. Mavris. Feasibility and benefit assessments of hybrid hydrogen fuel cell and battery configurations on a regional turboprop aircraft. In *AIAA AVIATION 2022 Forum*. American Institute of Aeronautics and Astronautics, June 2022.

DOI: 10.13009/EUCASS2025-453

[12] Clément Pornet, Corin Gologan, Patrick C. Vratny, Arne Seitz, Oliver Schmitz, Askin T. Isikveren, and Mirko Hornung. Methodology for sizing and performance assessment of hybrid energy aircraft. In *2013 Aviation Technology, Integration, and Operations Conference*. American Institute of Aeronautics and Astronautics, August 2013.

[13] C. Pornet, S. Kaiser, A.T. Isikveren, and M. Hornung. Integrated fuel-battery hybrid for a narrow-body sized transport aircraft. *Aircraft Engineering and Aerospace Technology*, 86(6):568–574, September 2014.

[14] Mark Voskuijl, Joris van Bogaert, and Arvind G. Rao. Analysis and design of hybrid electric regional turboprop aircraft. *CEAS Aeronautical Journal*, 9(1):15–25, October 2017.

[15] Air Transport Action Group. Waypoint 2050, second edition, 2021. Available onine: https://aviationbenefits.org/media/167417/w2050_v2021_27sept_full.pdf (accessed on 08 October 2024).

[16] Jürgen Thorbeck. Doc-assessment method, 2013. Available online: https://www.fzt.haw-hamburg.de/pers/Scholz/Aero/TU-Berlin_DOC-Method_with_remarks_13-09-19.pdf (accessed on 06 June 2025).

[17] Cedric Y. Justin, Alexia P. Payan, Simon I. Briceno, Brian J. German, and Dimitri N. Mavris. Power optimized battery swap and recharge strategies for electric aircraft operations. *Transportation Research Part C: Emerging Technologies*, 115:102605, June 2020.

[18] Patrick Ratei, Nabih Naeem, Prajwal Shiva Prakasha, and Björn Nagel. Sensitivity analysis of urban air mobility aircraft design and operations including battery charging and swapping. *CEAS Aeronautical Journal*, 15(4):1–15, April 2024.

[19] Air New Zealand. zero emissions aircraft, 2021. Available onine: https://p-airnz.com/cms/assets/PDFs/2021-air-nz-zero-emissions-aircraft-prd.pdf (accessed on 08 May 2025).

[20] Fuel Cells and Hydrogen 2 Joint Undertaking. *Hydrogen-powered aviation: a fact based study of hydrogen technology, economics, and climate impact by 2050.* Publications Office, 2020.

[21] Dominik Eisenhut, Nicolas Moebs, Evert Windels, Dominique Bergmann, Ingmar Geiß, Ricardo Reis, and Andreas Strohmayer. Aircraft requirements for sustainable regional aviation. *Aerospace*, 8(3):61, February 2021.

[22] Mansoor Mirza. *Economic Impact ofAirplane Turn-Times*. Boeing Aero Magazine, 2008.

[23] Andreas Schlegel. *Bodenabfertigungsprozesse im Luftverkehr*. Gabler, 2010.

[24] Hartmut Fricke and Michael Schultz. Improving aircraft turn around reliability. In *Third International Conference on Research in Air Transportation*, 2008.

[25] Michael Schmidt. A review of aircraft turnaround operations and simulations. *Progress in Aerospace Sciences*, 92:25–38, July 2017.

[26] Sara Sanz de Vicente. Ground handling simulation with cast. Master's thesis, Hamburg University of Applied Science, 2010.

[27] European Union Aviation Safety Agency. Easy access rules for air operations (regulation (eu) no 965/2012) revision 21, september 2023, 2023.

[28] Christopher J. Chuck and Joseph Donnelly. The compatibility of potential bioderived fuels with jet a-1 aviation kerosene. *Applied Energy*, 118:83–91, apr 2014.

[29] Coordinating Research Council. *Handbook of Aviation Fuel Properties*. CRC Report No. 530, Atlanta, Georgia, 1983.

[30] Nathan Gray, Shane McDonagh, Richard O'Shea, Beatrice Smyth, and Jerry D Murphy. Decarbonising ships, planes and trucks: An analysis of suitable low-carbon fuels for the maritime, aviation and haulage sectors. *Advances in Applied Energy*, 1:100008, feb 2021.

[31] Marina Braun-Unkhoff and Uwe Riedel. Alternative fuels in aviation. *CEAS Aeronautical Journal*, 6(1):83–93, sep 2014.

DOI: 10.13009/EUCASS2025-453

[32] Eduardo Cabrera and João M. Melo de Sousa. Use of sustainable fuels in aviation—a review. *Energies*, 15(7):2440, mar 2022.

[33] Joshua Heyne, Bastian Rauch, Patrick Le Clercq, and Meredith Colket. Sustainable aviation fuel prescreening tools and procedures. *Fuel*, 290:120004, apr 2021.

[34] Christiane Voigt, Jonas Kleine, Daniel Sauer, Richard H. Moore, Tiziana Bräuer, Patrick Le Clercq, Stefan Kaufmann, Monika Scheibe, Tina Jurkat-Witschas, Manfred Aigner, Uwe Bauder, Yvonne Boose, Stephan Borrmann, Ewan Crosbie, Glenn S. Diskin, Joshua DiGangi, Valerian Hahn, Christopher Heckl, Felix Huber, John B. Nowak, Markus Rapp, Bastian Rauch, Claire Robinson, Tobias Schripp, Michael Shook, Edward Winstead, Luke Ziemba, Hans Schlager, and Bruce E. Anderson. Cleaner burning aviation fuels can reduce contrail cloudiness. *Communications Earth & Environment*, 2(1), jun 2021.

[35] B. W. Kolosz, Y. Luo, B. Xu, M. M. Maroto-Valer, and J. M. Andresen. Life cycle environmental analysis of 'drop in' alternative aviation fuels: a review. *Sustainable Energy & Fuels*, 4(7):3229–3263, 2020.

[36] Airbus S.A.S. A320 Aircraft Characteristics - Airport and Maintenance Planning, 2020.

[37] American Petroleum Institure. Protection Against Ignitions Arising Out of Static, Lightning, and Stray Currents. API RP 2003, 1998.

[38] Anup Sera. Jet Fuel Pipelines And Storage Require Special Operation, Maintenance Considerations. *Pipeline & Gas Journal*, 2009.

[39] A. Kazda and Robert E. Caves. *Airport Design and Operation*. Emerald Group Publishing Limited, 2015.

[40] Jonas Mangold, Daniel Silberhorn, Nicolas Moebs, Niclas Dzikus, Julian Hoelzen, Thomas Zill, and Andreas Strohmayer. Refueling of LH2 aircraft—assessment of turnaround procedures and aircraft design implication. *Energies*, 15(7):2475, mar 2022.

[41] J E Jensen, W A Tuttle, R B Stewart, H Brechna, and A G Prodell. *Brookhaven National Laboratory selected cryogenic data notebook: Volume 1, Sections 1-9*. Brookhaven National Laboratory, USA, 1980.

[42] E. W. Lemmon, I. H. Bell, M. L. Huber, and M. O. McLinden. NIST Standard Reference Database 23: Reference Fluid Thermodynamic and Transport Properties-REFPROP, Version 10.0, National Institute of Standards and Technology, 2018.

[43] Manfred Klell, Helmut Eichlseder, and Alexander Trattner. *Wasserstoff in der Fahrzeugtechnik*. Springer Fachmedien Wiesbaden, 2018.

[44] J. Hord. Selected topics on hydrogen fuel: Nbsir 75-803. *National Bureau of Standards*, 1975.

[45] Jacob W. Leachman, Richard T Jacobsen, Eric W. Lemmon, and Steven G. Penoncello. *Thermodynamic Properties of Cryogenic Fluids*. Springer International Publishing, 2017.

[46] D. Verstraete, P. Hendrick, P. Pilidis, and K. Ramsden. Hydrogen fuel tanks for subsonic transport aircraft. *International Journal of Hydrogen Energy*, 35(20):11085–11098, oct 2010.

[47] Sandeep Kumar Dwivedi and Manish Vishwakarma. Hydrogen embrittlement in different materials: A review. *International Journal of Hydrogen Energy*, 43(46):21603–21616, nov 2018.

[48] G. Daniel Brewer. *Hydrogen Aircraft Technology*. Routledge, 1 edition, 1991.

[49] J. Hoelzen, M. Flohr, D. Silberhorn, J. Mangold, A. Bensmann, and R. Hanke-Rauschenbach. H2-powered aviation at airports – design and economics of lh2 refueling systems. *Energy Conversion and Management: X*, 14:100206, May 2022.

[50] Julian Hoelzen. *Hydrogen-powered aviation – techno-economics of flying with green liquid hydrogen*. PhD thesis, Gottfried Wilhelm Leibniz Universität Hannover, 2024.

[51] J. Hoelzen, D. Silberhorn, F. Schenke, E. Stabenow, T. Zill, A. Bensmann, and R. Hanke-Rauschenbach. H2-powered aviation – optimized aircraft and green lh2 supply in air transport networks. *Applied Energy*, 380:124999, February 2025.

DOI: 10.13009/EUCASS2025-453

[52] Jonas Mangold. Economical assessment of hydrogen short-range aircraft with the focus on the turnaround procedure. Master's thesis, University of Stuttgart. Germany, 2021.

[53] Inga Beyers, Astrid Bensmann, and Richard Hanke-Rauschenbach. Ragone plots revisited: A review of methodology and application across energy storage technologies. *Journal of Energy Storage*, 73, 2023.

[54] Sven Wiegelmann, Astrid Bensmann, and Richard Hanke-Rauschenbach. Performance characterization of lithium-ion battery cells within restricted operating range using an extended ragone plot. *Applied Energy*, 389:125704, July 2025.

[55] Heide Budde-Meiwes, Julia Drillkens, Benedikt Lunz, Jens Muennix, Susanne Rothgang, Julia Kowal, and Dirk Uwe Sauer. A review of current automotive battery technology and future prospects. *Proceedings of the Institution of Mechanical Engineers, Part D: Journal of Automobile Engineering*, 227(5):761–776, apr 2013.

[56] Patrick Christoph Vratny. *Conceptual Design Methods of Electric Power Architectures for Hybrid Energy Aircraft*. PhD thesis, Technische Universität München, 2019.

[57] Zachary Heit and Susan Liscouet-Hanke. Estimation of battery pack layout and dimensions for the conceptual design of hybrid-electric aircraft. In *AIAA SCITECH 2023 Forum*. American Institute of Aeronautics and Astronautics, January 2023.

[58] D. Bernardi, E. Pawlikowski, and J. Newman. A general energy balance for battery systems. *Journal of The Electrochemical Society*, 132(1):5–12, jan 1985.

[59] Zeyang Geng, Jens Groot, and Torbjorn Thiringer. A time- and cost-effective method for entropic coefficient determination of a large commercial battery cell. *IEEE Transactions on Transportation Electrification*, 6(1):257–266, March 2020.

[60] Guangming Liu, Minggao Ouyang, Languang Lu, Jianqiu Li, and Xuebing Han. Analysis of the heat generation of lithium-ion battery during charging and discharging considering different influencing factors. *Journal of Thermal Analysis and Calorimetry*, 116(2):1001–1010, January 2014.

[61] Chunrong Zhao, Juan Rasines Mazo, and Dries Verstraete. Optimisation of a liquid cooling system for evtol aircraft: Impact of sizing mission and battery size. *Applied Thermal Engineering*, 246:122988, June 2024.

[62] Agata Kuśmierek, Cezary Galiński, and Wieńczysław Stalewski. Review of the hybrid gas - electric aircraft propulsion systems versus alternative systems. *Progress in Aerospace Sciences*, 141:100925, August 2023.

[63] Benjamin J. Brelje and Joaquim R.R.A. Martins. Electric, hybrid, and turboelectric fixed-wing aircraft: A review of concepts, models, and design approaches. *Progress in Aerospace Sciences*, 104:1–19, January 2019.

[64] Federal Aviation Administration. Airworthiness criteria: Special class airworthiness criteria for the amazon.com services llc mk27–2 unmanned aircraft; correction, 2022. Available onine: https://www.govinfo.gov/content/pkg/FR-2022-02-24/pdf/2022-03778.pdf (accessed on 08 May 2025).

[65] Sunghun Jung and Hyunsu Kim. Analysis of amazon prime air uav delivery service. *Journal of Knowledge Information Technology and Systems*, 2017.

[66] Koji A. O. Suzuki, Paulo Kemper Filho, and James R. Morrison. Automatic battery replacement system for uavs: Analysis and design. *Journal of Intelligent & Robotic Systems*, 65(1–4):563–586, September 2011.

[67] Len Schumann. *Reduktion des Energiebedarfs mittels einesbatterieelektrischen Antriebsam Beispiel eines Kleinugzeugs*. PhD thesis, University of Stuttgart, 2018.

[68] R F Nanda, M P Nugraha, C An, and D E Cahyanti. Comparison of the effectiveness and efficiency on cessna 208 with dhc 6-300 twin otter for flights in inland papua. *Journal of Physics: Conference Series*, 1573(1):012029, July 2020.

[69] Avions de Transport Regional. Atr 42-500: Flight crew operating manual, 1998.

[70] Philip Balack, Georgi Atanasov, and Thomas Zill. Architectural trade-offs for a hybrid-electric regional aircraft. In *Proceedings of the Aerospace Europe Conference - EUCASS - CEAS - 2023*. Proceedings of the Aerospace Europe Conference - EUCASS - CEAS - 2023, 2023.

DOI: 10.13009/EUCASS2025-453

[71] Furkan Ahmad, Mohammad Saad Alam, Ibrahim Saad Alsaidan, and Samir M. Shariff. Battery swapping station for electric vehicles: opportunities and challenges. *IET Smart Grid*, 3(3):280–286, May 2020.

[72] Xi Chen, Kai Xing, Feng Ni, Yujie Wu, and Yongxiang Xia. An electric vehicle battery-swapping system: Concept, architectures, and implementations. *IEEE Intelligent Transportation Systems Magazine*, 14(5):175–194, September 2022.

[73] Yusheng Zhang. Analysis of battery swapping technology for electric vehicles – using nio's battery swapping technology as an example. *SHS Web of Conferences*, 144:02015, 2022.

[74] Sebastian Rivera, Stefan M. Goetz, Samir Kouro, Peter W. Lehn, Mehanathan Pathmanathan, Pavol Bauer, and Rosa Anna Mastromauro. Charging infrastructure and grid integration for electromobility. *Proceedings of the IEEE*, 111(4):371–396, April 2023.

[75] Abdilbari Shifa Mussa, Matilda Klett, Mårten Behm, Göran Lindbergh, and Rakel Wreland Lindström. Fast-charging to a partial state of charge in lithium-ion batteries: A comparative ageing study. *Journal of Energy Storage*, 13:325–333, October 2017.

[76] Kailong Liu, Kang Li, Qiao Peng, and Cheng Zhang. A brief review on key technologies in the battery management system of electric vehicles. *Frontiers of Mechanical Engineering*, 14(1):47–64, April 2018.

[77] Yawen Liang, Gautham Ram Chandra Mouli, and Pavol Bauer. Charging technology for electric aircraft: State of the art, trends, and challenges. *IEEE Transactions on Transportation Electrification*, 10(3):6761–6788, September 2024.

[78] Yawen Liang, Dávid Bodnár, Gautham Ram Chandra Mouli, Daniele Ragni, and Pavol Bauer. Charging demand prediction: Small all-electric aircraft and electric vertical takeoff and landing aircraft. *IEEE Transactions on Transportation Electrification*, 11(1):2732–2747, February 2025.

[79] Soo Seok Choi and Hong S Lim. Factors that affect cycle-life and possible degradation mechanisms of a li-ion cell based on licoo2. *Journal of Power Sources*, 111(1):130–136, September 2002.

[80] Peng Zhang, Jun Liang, and Feng Zhang. An overview of different approaches for battery lifetime prediction. *IOP Conference Series: Materials Science and Engineering*, 199:012134, May 2017.

[81] Hao Tu, Hao Feng, Srdjan Srdic, and Srdjan Lukic. Extreme fast charging of electric vehicles: A technology overview. *IEEE Transactions on Transportation Electrification*, 5(4):861–878, December 2019.

[82] Federal Aviation Administration. 14 CFR Part 43 – Maintenance, Preventive Maintenance, Rebuilding, and Alteration. Available online: https://www.ecfr.gov/current/title-14/chapter-I/subchapter-C/part-43 (accessed on 04 June 2025).

[83] Federal Aviation Administration. 14 CFR Part 125 – Certification and Operations: Airplanes Having a Seating Capacity of 20 or More Passengers or a Maximum Payload Capacity of 6,000 Pounds or More. Available online: https://www.ecfr.gov/current/title-14/chapter-I/subchapter-G/part-125 (accessed on 04 June 2025).

[84] Federal Aviation Administration. 14 CFR Part 91 – General Operating and Flight Rules. Available online: https://www.ecfr.gov/current/title-14/chapter-I/subchapter-F/part-91 (accessed on 04 June 2025).

[85] International Organization for Standardization. ISO 11228-1:2021(en)Ergonomics – Manual handling – Part 1: Lifting, lowering and carrying, 2021.

[86] Bundesanstalt rür Arbeitsschutz und Arbeitsmedizin. Manuelles heben, halten und tragen. 2022.

[87] Heinrich Mensen. *Handbuch der Luftfahrt*. Springer Berlin Heidelberg, 2013.

[88] IL5000 Hubtisch 5000kg. Available online: https://saxlift.com/de/hubtische/einfachscherenhubtische/il5000 (accessed on 05 June 2025).

[89] Technische Regeln für Gefahrstoffe TRGS 720 Gefährliche explosionsfähige Gemische—Allgemeines, 2020. Available online: https://www.baua.de/DE/Angebote/Rechtstexte-und-Technische-Regeln/Regelwerk/TRGS/pdf/TRGS-720.pdf?__blob=publicationFile&v=5 (accessed on 14 October 2020).

DOI: 10.13009/EUCASS2025-453

[90] Technische Regeln für Betriebssicherheit/ Gefahrstoffe TRBS 2151 Teil 1/ TRGS 721 Gefährliche explosionsfähige Atmosphäre—Beurteilung der Explosionsgefährdung, 2006. Available online: https://www.baua.de/DE/Angebote/Rechtstexte-und-Technische-Regeln/Regelwerk/TRGS/pdf/TRGS-721.pdf?__blob=publicationFile&v=6 (accessed on 01 October 2020).

[91] National Fire Protection Association. Standard for Aircraft Fuel Servicing. *NFPA 407*, 2001.

[92] Richtlinie 2014/34/EU des Europäischen Parlaments und des Rates vom 26. Februar 2014 zur Harmonisierung der Rechtsvorschriften der Mitgliedstaaten für Geräte und Schutzsysteme zur bestimmungsgemäßen Verwendung in explosionsgefährdeten Bereichen (Neufassung). Avaiable online: https://eur-lex.europa.eu/legal-content/DE/ALL/?uri=celex%3A32014L0034 (accessed on 12 November 2020).

[93] Richtlinie 1999/92/EG des Europäischen Parlaments und des Rates vom 16. Dezember 1999 über Mindestvorschriften zur Verbesserung des Gesundheitsschutzes und der Sicherheit der Arbeitnehmer, die durch explosionsfähige Atmosphären gefährdet werden können (Fünfzehnte Einzelrichtlinie im Sinne von Artikel 16 Absatz 1 der Richtlinie 89/391/EWG). Available online: https://eur-lex.europa.eu/legal-content/DE/ALL/?uri=CELEX:31999L0092 (accessed on 12 November 2020).

[94] Jonas Mangold, Dominik Eisenhut, Felix Brenner, Nicolas Moebs, and Andreas Strohmayer. Preliminary hybrid-electric aircraft design with advancements on the open-source tool SUAVE. In *Journal of Physics: Conference Series*, volume 2526, 2023.

[95] Jonas Mangold and Andreas Strohmayer. Preliminary aircraft design for hybrid electric propulsion architectures: A focus on critical loss of thrust. *Aerospace*, 12(4):275, March 2025.

[96] Timothy MacDonald, Matthew Clarke, Emilio M. Botero, Julius M. Vegh, and Juan J. Alonso. Suave: An open-source environment enabling multi-fidelity vehicle optimization. In *18th AIAA/ISSMO Multidisciplinary Analysis and Optimization Conference*. American Institute of Aeronautics and Astronautics, June 2017.

[97] Emilio M. Botero, Andrew Wendorff, Timothy MacDonald, Anil Variyar, Julius M. Vegh, Trent W. Lukaczyk, Juan J. Alonso, Tarik H. Orra, and Carlos Ilario da Silva. Suave: An open-source environment for conceptual vehicle design and optimization. In *54th AIAA Aerospace Sciences Meeting*. American Institute of Aeronautics and Astronautics, January 2016.

[98] Reynard de Vries, Malcom Brown, and Roelof Vos. Preliminary sizing method for hybrid-electric distributed-propulsion aircraft. *Journal of Aircraft*, 56(6):2172–2188, November 2019.

[99] Laurent Bovet. Conceptual design optimization of hybrid-electric regional aircraft using spph architecture. In *Proceedings of the Aerospace Europe Conference - EUCASS - CEAS - 2023*, 2023.

[100] D. Eisenhut, J. Mangold, N. Moebs, F. Brenner, and A. Strohmayer. Case study on hybrid-electric aircraft designs enabled by an enhanced suave version. *Journal of Physics: Conference Series*, 2526(1):012019, June 2023.

[101] Deutsches Institut für Normung (DIN) and Verband der Elektrotechnik (VDE). Din vde 0100-410: Low-voltage electrical installations – part 4-41: Protection for safety - protection against electric shock. German Standard DIN VDE 0100-410:2018-10, 2018. Berlin, Germany.

[102] International Electrotechnical Commission (IEC). IEC 61140: Protection Against Electric Shock – Common Aspects for Installation and Equipment. International Standard IEC 61140:2016, 2016.

[103] Gerhard Kiefer, Herbert Schmolke, and Karsten Callondann. *VDE 0100 und die Praxis: Wegweiser für Elektrofachkräfte*. VDE Verlag, Berlin, 2024.

[104] Zhi-Ning Liu, Xia-Qing Liu, Lu-Jian Yang, David Leo, and Hong-Wei Zhao. An autonomous dock and battery swapping system for multirotor uav. 2018.

[105] Amrit Kumar Thakur, Ravishankar Sathyamurthy, R. Velraj, R. Saidur, A.K. Pandey, Z Ma, Punit Singh, Soumya Kanti Hazra, Swellam Wafa Sharshir, Rajendran Prabakaran, Sung Chul Kim, Satyam Panchal, and Hafiz Muhammad Ali. A state-of-the art review on advancing battery thermal management systems for fast-charging. *Applied Thermal Engineering*, 226:120303, May 2023.

[106] Joby Aviation. Global Electric Aviation Charging System (GEACS), 2023. Available online: https://joby-site.cdn.prismic.io/joby-site/5f82ea34-645e-4468-8e3f-14a16e298941_Joby-Charging-GEACS-final.pdf (accessed on 04 June 2025).